

Manufacture of Local Dental Porcelain from Mesopotamian Rocks and Evaluation of Adding Na_2CO_3 in Different Proportions on Its Physical and Mechanical Properties

Firas H. Alwade ^{1*}, Shihab A. Zaidan ²

^{1*} Al-Mustansiriya University, College of Dentistry, Baghdad, 11001, Iraq.

² University of Technology, Department of Applied Sciences, Baghdad, 10001, Iraq.

¹firasalwadephysics@uomustansiriyah.edu.iq, ²Shihab.A.Zaidan@uotechnology.edu.iq.

Abstract

The research offers inexpensive, Iraqi-accessible, and high-quality alternative raw materials for porcelain used in dental and bone implants that are suitable for their production. In addition to other porcelain oxides (CaO , K_2O , SiO_2 , Al_2O_3 , B_2O_3), which may be found in some raw clay materials, the use of soda carbonate (Na_2CO_3) as a binding material is also employed. The measurement of porosity, density, diametrical strength, hardness, and thermal expansion coefficient showed a decrease in porosity and an increase in density, diametrical strength, hardness, and thermal expansion coefficient with an increase in soda carbonate percentage. This means the soda carbonates are forming glass phases to bond the granules with each other and increase the convergence between the granulose boundaries and close the internal spaces.

Keywords: Porcelain, Feldspar, apparent density, thermal expansion.

Article history: Received: 28 Aug. 2025, Accepted: 29 Sep. 2025, Published: 01 Dec. 2025

This article is open-access under the CC BY 4.0 license (<http://creativecommons.org/licenses/by/4.0/>).

1. Introduction

The considered clay products are the earliest patterns of human industry [1]. Historically, ceramic products were made completely or partly from clays that were heat-treated at high temperatures to obtain the required hardness [2]. Scientific and technical development led to the development of the ceramic definition, and it became known as a product made from a material or mixture of inorganic and non-metallic materials by heat treatment [3].

The advancement of ceramic materials and heat treatment techniques has resulted in their application in biological fields, leading to the term "biological ceramics" [4]. It's utilized in dentistry as ceramic (porcelain) for the production of complete and partial dentures, as well as for creating artificial teeth in both complete and partial denture crowns and inner restorations, filling as well as single teeth, upper and lower crowns, inlay and onlay restorations [5].

Porcelain is a specialized ceramic material used in the dental industry. It is sometimes referred to as "Chinese Porcelain" or "White Products," and is recognized as the purest form of traditional ceramic compounds [6]. Traditional porcelain is prepared by firing a mixture of kaolin, quartz, and feldspar [7]. Kaolin is composed of the

union of two layers. The first is known as the silica layer, which consists of silicon and oxygen atoms, and the second is known as the gypsum layer, which consists of aluminum atoms and hydroxyl groups. The pure metal contains 39.5% aluminum oxide and 46.5% silicon oxide, and it also contains 14% crystalline water [8]. In Iraq, the Ka'ara Depression in the Western Desert is the most important location where kaolin deposits are concentrated [9].

2. Materials and Methods

2.1 Raw Materials Powder Preparation

Kaolin ($\text{Al}_2\text{O}_3 \cdot 2\text{SiO}_2 \cdot 2\text{H}_2\text{O}$) with (99.9%) purity ((Fluka AG), Potassium feldspar (Iraqi General Company for Geological Survey), Boron Oxides (B_2O_3), Aluminum Oxide (Al_2O_3), Calcium Oxide (CaO) with (99.9%) purity ((Fluka AG) and Non-aqueous sodium carbonate (Na_2CO_3) with (99.9%) purity from (Agfa) are used as raw materials for preparing porcelain mixtures.

2.2 Dental Porcelain Mixture Preparation

The components of dental porcelain and alumina core type percentages were chosen according to the specifications used globally in this field [10], as shown in Table 1 below.

Table 1: Metal oxides percentages in the porcelain mixture used in the dental industry.

| Oxide Type | Wt. % |
|--------------------------------|-------|
| SiO ₂ | 35.0 |
| Al ₂ O ₃ | 53.8 |
| CaO | 1.12 |
| Na ₂ O | 2.68 |
| K ₂ O | 4.2 |
| B ₂ O ₃ | 3.2 |

To complete the dental porcelain mixture, Na₂O was required. Since it is not available, it was replaced with Na₂CO₃, which was added to the mixtures in the following manner, as shown in Table 2:

Table 2: Proportions of mixtures prepared from dental porcelain

| Mix Symbol | Na ₂ CO ₃ % | Remaining Materials% |
|------------|-----------------------------------|----------------------|
| A | 0 | 100 |
| B | 2 | 98 |
| C | 4 | 96 |
| D | 6 | 94 |
| E | 8 | 92 |
| F | 10 | 90 |

2.3 Mixing, Grinding & Sieving Process:

The six mixtures were mixed and ground in a homemade ball mill, using ceramic balls that rotate. The mixtures were placed for 5 hours, then sieved to achieve a particle size of less than (53) μm.

2.4 Preparation of Sample Process

In quantities of (10, 8, 6, 4, 2, 0)%, Na₂CO₃ was added to six dental porcelain mixes.

2.5 Forming & Drying Process

Samples were prepared using a semi-dry pressing method with a hydraulic press and steel mold. After shaping, they were dried naturally in the air for 24 hours and then in an electric dryer at 50°C for four hours.

2.6 Sintering Process

The sintering process involved raising a Carbolite furnace temperature at a rate of 50 degrees every half hour until it reached 300°C. The temperature was then raised to 400°C and 500°C to remove crystallization water. The model was then kept in the oven for one and a half hours to complete the sintering process.

2.7 Physical Properties test

- **Apparent Porosity and Water Absorption**

After the sintering process, the samples were weighed dry using a German Sartorius balance with a 0.01 g sensitivity. The apparent porosity and water absorption of the samples are calculated using equation (1).

$$A.P = \frac{W_2 - W_1}{W_2 - W_3} \text{-----(1)}$$

Where A. Pis apparent porosity and W₁, W₂ and W₃ are sintered weight, soaked weight and suspended weight of the sample, respectively [11].

- **Density**

Samples are sintered, weighed dry, immersed in distilled water, weighed submerged, cleaned, and weighed again. Their apparent density is calculated using Archimedes' principle, using relation (2). The process involves removing surface water and absorbing internal water.

$$A.D. = \frac{W_d}{W_d - W_i} \text{----- (2)(12)}$$

Where: A.D: Apparent density; w_d: The weight of the sample when dry and W_i: The weight of the sample when is immersed in distilled water.

2.8 Mechanical Properties Test

- **Diametrical Strength**

The model and components of the axial fracture toughness testing system are shown in Fig. 1 below. The result can be derived using equation (3).

$$\text{Diametrical Strength } \sigma_D = \frac{2F}{\pi Dt} \text{-----(3)(13, 14)}$$

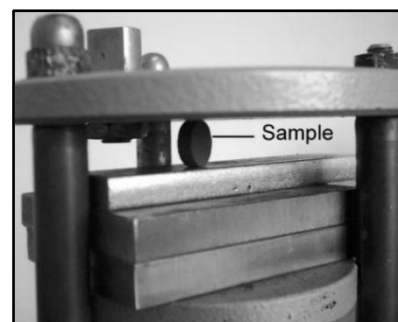


Fig. 1 Axial fracture system.

Where: F: represents the maximum applied load in Newtons (N), D is the measured diameter of the sample in milli-meters (mm) and t is the measured length of the sample (mm)

- **Hardness Test**

The hardness test was conducted using the Vickers method and a digital hardness tester model XCHL-11A Multi-function HI-sclerometer, produced by Huizhouchangliu-Hi-Tech Co., Ltd., of Chinese origin.

2.9 Thermal Properties Test

• Thermal Expansion

The linear thermal expansion measurement system is illustrated in Fig. 2, where the percentage of thermal expansion is calculated using Equation (4):

$$\begin{aligned} \text{Expansion\%} &= \frac{\text{Total Expansion}}{\text{Length of test piece}} \times 100 \% \\ &= \frac{\Delta L}{L_0} 100\% \text{ ---- (4)} \end{aligned}$$

Thermal expansion percentage is calculated at different temperatures, and the coefficient of thermal expansion is calculated from relation (5).

$$\frac{\Delta l}{l_0} = \alpha_1 \Delta T \text{ ---- (5)}$$

Where: α_1 : Linear Thermal Expansion Coefficient [15].

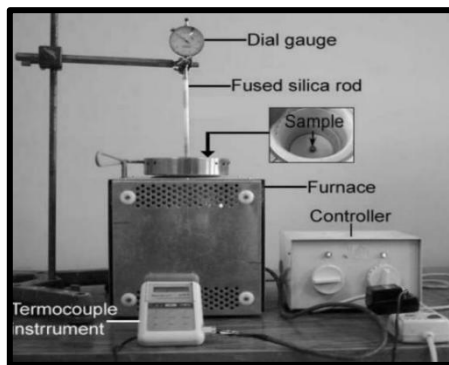


Fig. 2 Linear thermal expansion measurement system.

• Surface Microstructure

Surface composition of manufactured samples was examined using a Nikon optical microscope after polishing with artificial silicon carbide discs at 1200°C, cleaning with hydrofluoric acid, washing with water, drying, and examining under the microscope.

3. Results

In this section, the results of the study are displayed and discussed in detail. However, Fig. 3 showed that, compared to samples without added sodium carbonate, porosity decreases as the quantity of Na₂CO₃ increases, reaching extremely low values at high percentages (10%) of Na₂CO₃.

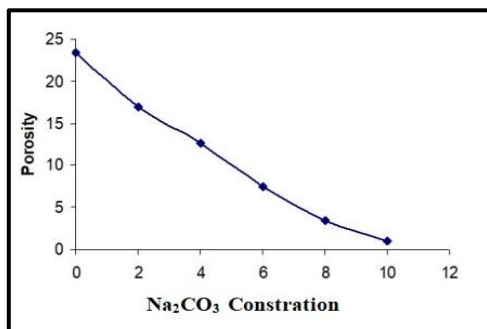


Fig. 3 Change in porosity with the change in Na₂CO₃ concentration

The results in Fig. 4 demonstrate that, despite the little shrinkage in dimensions caused by burning, which varied from 8.48 percent for mixture A to 9.27 percent for mixture F.

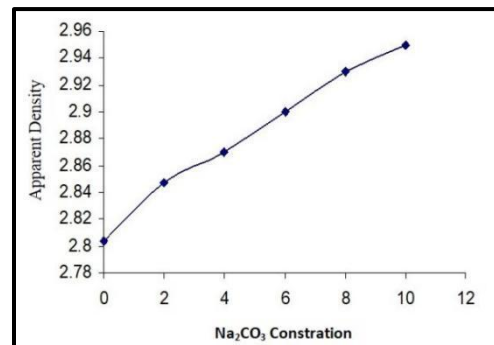


Fig. 4 Change in apparent density with Change in Na₂CO₃ concentration.

While Fig. 5 displayed an increased in hardness with increased in Na₂CO₃ concentration.

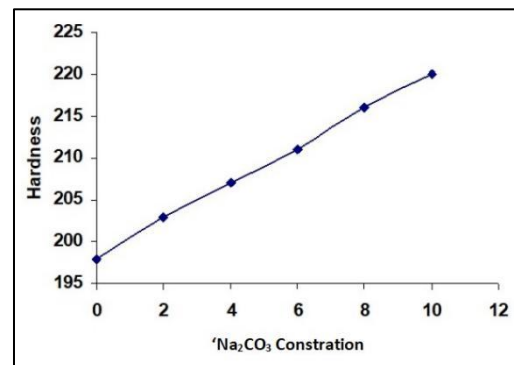


Fig. 5 Change in hardness with Change in Na₂CO₃ concentration.

Likewise, Fig. 6 showed an increase in axial fracture toughness with the increasing proportion of added Na₂CO₃, which means an enhancement in tensile and compressive properties since this type of testing involves tensile and compressive resistance.

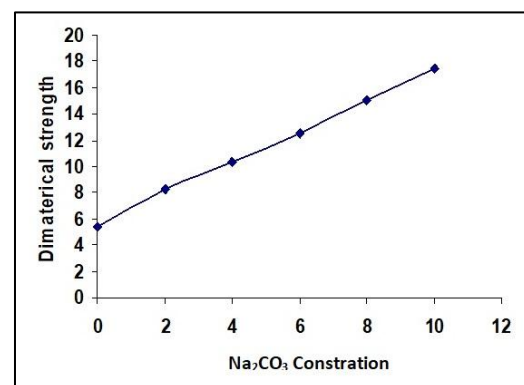


Fig. 6 Change in diametrical strength with Change in Na₂CO₃ concentration.

Furthermore, all of the Figs. (7, 8, 9, 10, 11, 12) illustrated the change in the percentage of linear thermal expansion with the change in temperature from 50°C to

850°C, where we observed an increase in the percentage of thermal expansion with the increase in temperature for the Na₂CO₃ samples (10, 8, 6, 4, 2, 0%).

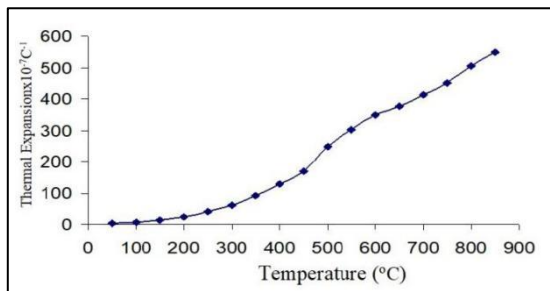


Fig. 7 Change in the percentage of linear thermal expansion with the change in temperature for mixed (A).

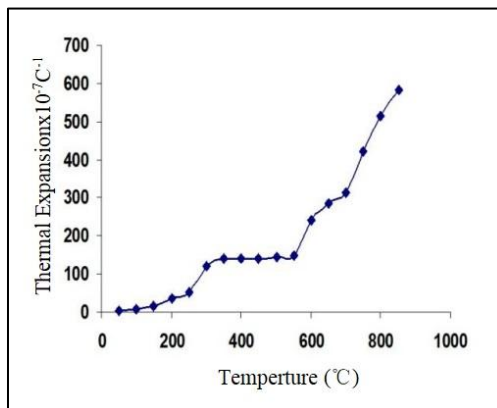


Fig. 10 Change in the percentage of linear thermal expansion with the change in temperature for mixed (D).

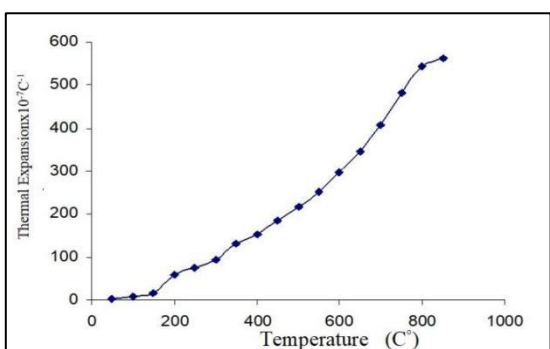


Fig. 8 Change in the percentage of linear thermal expansion with the change in temperature for mixed (B).

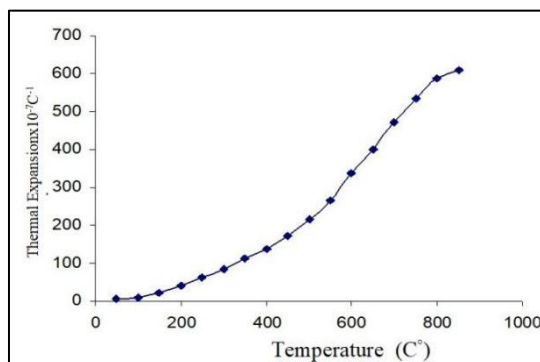


Fig. 11 Change in the percentage of linear thermal expansion with the change in temperature for mixed (E).

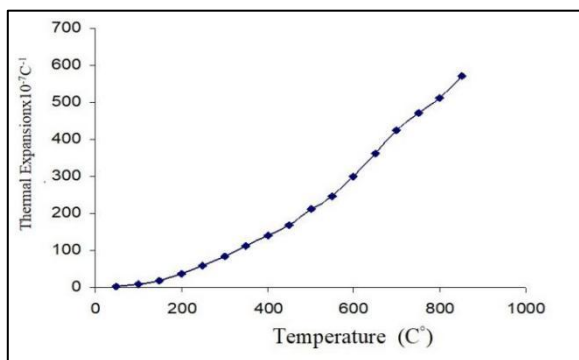


Fig. 9 Change in the percentage of linear thermal expansion with the change in temperature for mixed (C).

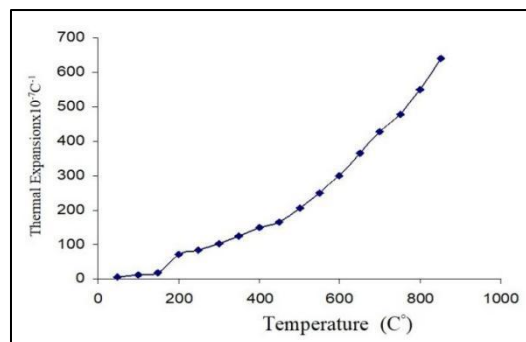


Fig. 12 The change in the percentage of linear thermal expansion with the change in temperature for mixed (F).

Fig. 13 explains the change in the thermal expansion coefficient with the added percentage of Na₂CO₃.

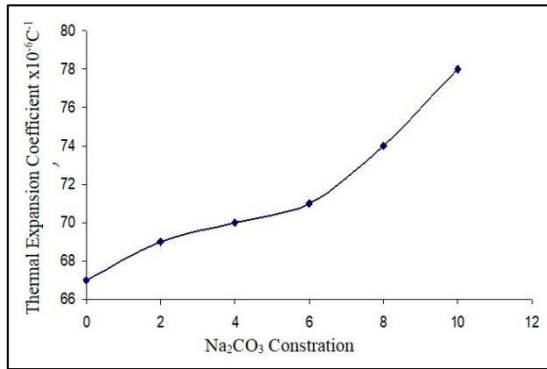


Fig. 13 The change in the thermal expansion coefficient with the addition of Na₂CO₃.

The images in figures (14a, b, c, d, e, f) taken using an optical microscope of the sample surfaces show that the samples with added (0, 2, 4, 6%) Na₂CO₃ have a highly homogeneous surface, while the samples with added (8, 10%) Na₂CO₃ exhibit significant inhomogeneity on the sample surface.

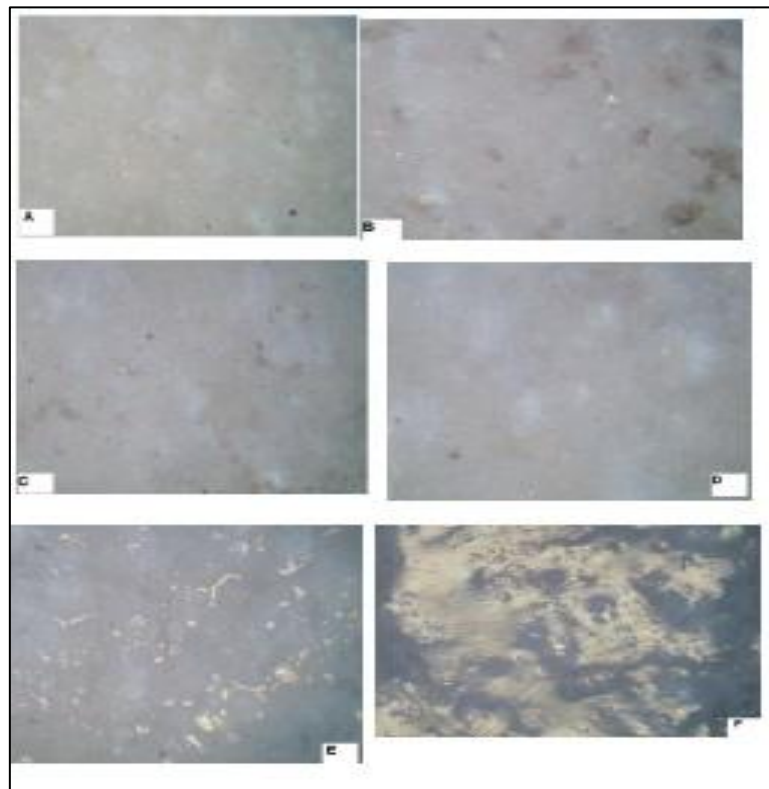


Fig. 14 The images (A, B, C, D, E and F) display scanning electron microscope images of porcelain bodies with mixtures F, E, D, C, B, A.

X-ray diffraction tests on porcelain samples in figures 15a and 15b before and after burned revealed a decrease in the mullite phase, boron silicate phase, and albite phase.

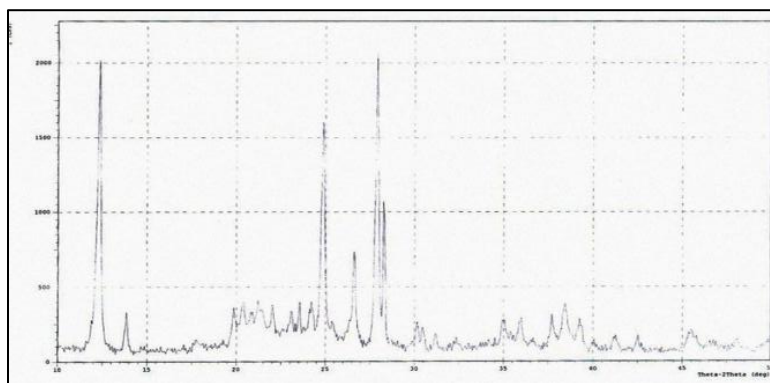


Fig. 15 b: The X-ray diffraction pattern of the porcelain body of the mixture before burning(C)

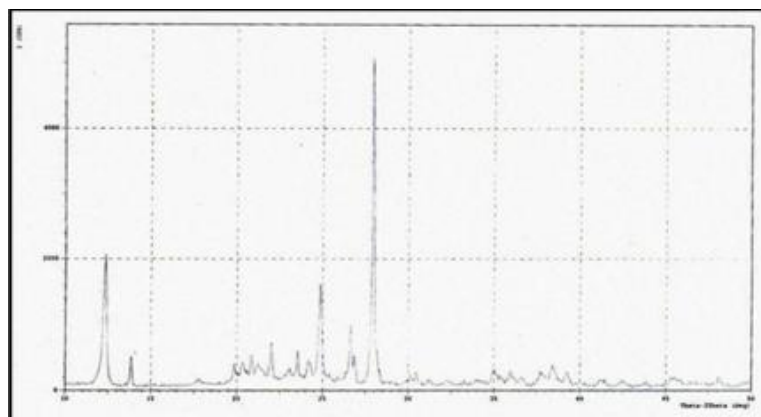


Fig. 15a The X-ray diffraction pattern of the porcelain body of the mixture after burning(C).

4. Discussion

The decrease in porosity in Fig. 3 is attributed to the fact that the sodium oxide is created when Na_2CO_3 is burned with other oxides to form molten glassy phases that bond the grain boundaries of oxides that are more heat-resistant, like alumina. Consequently, there is a significant convergence between the grains, which helps to fill the pores and interstitial gaps. The percentage of molten phases increases with the addition of Na_2CO_3 , despite the formation of voids due to the release of carbon dioxide.

While the apparent density in the Figs. related to Na_2CO_3 increases because of the significant decrease in porosity. As a result of Fig. 4, the density ranged between 2.8 and 2.95, which is a suitable range for dental material.

However, the porosity decrease was clear, and the release of CO_2 may lead to the appearance of microscopic defects, especially if there is a granular convergence that prevents the gas from scampering freely. Therefore, high compression forces were avoided on the samples, and this may negatively affect crystal growth.

Hardness is the resistance to permanent indentation or penetration and is considered a second predictor of the mechanical properties of dental materials [16]. As for the change in hardness with the addition of Na_2CO_3 , it was observed from fig. 5 that the hardness increased with the increase in the amount of added Na_2CO_3 due to the

significant reduction in apparent porosity, which greatly affects the ceramic body's resistance to penetration. This means that high values of added Na_2CO_3 positively affect the hardness of these mixtures, as hardness is one of the important tests for dental materials because these materials may be subjected to point stresses during installation. Additionally, hardness determines the body's resistance to wear or abrasion. Therefore, the addition of Na_2CO_3 increased the ceramic material's resistance to wear, in addition to the importance of hardness in the case of re-grinding and crushing this mixture for use in dental constructions.

Fig. 6 also displayed an increase in axial fracture toughness with the increasing proportion of added Na_2CO_3 , which means an enhancement in tensile and compressive properties since this type of testing involves tensile and compressive resistance. The increase in compressive resistance represents an improvement in the ability of this porcelain material to withstand the compressive stresses that the tooth is subjected to during application. Despite the relatively low fracture toughness values due to the low force used to form the samples, which, if increased, could positively lead to an increase in fracture toughness.

The noticeable change of linear thermal expansion in Figs. (7, 8, 9, 10, 11, 12) is due to the thermal expansion beginning to stabilize at temperatures above 800°C . This

is attributed to the increased packing of the grains with each other and the decrease in porosity, where the grains expand with each other, resulting in thermal expansion from the sum of the grains aligned along one axis. In some curves, a relative stability in thermal expansion with increasing temperature was observed, which indicates that the material has reached a softening state in the nascent phase of sodium's reaction with other oxides. In general, the thermal expansion coefficient values ranged between ($67 \times 10^{-7} \text{C}^{-1}$) and ($78 \times 10^{-7} \text{C}^{-1}$), which are suitable values for conducting subsequent operations on this material without the occurrence of cracking and breaking.

Fig. 13 indicates that the thermal expansion coefficient increases with the increase in the percentage of Na_2CO_3 . The main reason for this increase is the higher density in the material, which causes the particles to pack more tightly and increases the expansion. However, the thermal expansion values for natural teeth range from ($100\text{-}150 \times 10^{-6} \text{C}^{-1}$) for temperatures between 20°C and 50°C . Thermal expansion plays a crucial role in determining the success of the glazing process and its compatibility with the components of the tooth structure. Therefore, the choice of the mixture and the percentage of added Na_2CO_3 depends on the type of other material and the thermal expansion coefficient, especially when performing structural operations on layers of teeth, particularly in the case of applying enamel coating on metal surfaces.

Figs. (14 a, b, c, d, e, f) shows the attributed to the increased glassy phase resulting from the higher sodium content, which usually appears clearly on the sample surfaces, leading to surface roughness. There is a possibility of dimensional distortion and inhomogeneity when the Na_2CO_3 content is increased to higher values or when the firing temperature is raised.

Fig. 15a and 15b, before and after burning, indicate a decrease in the phases due to a sodium oxide reaction from Na_2CO_3 combustion, making it difficult to determine all because of the porcelain composition. Anorthoclase, a common phase between sodium and potassium, appeared with the formula $(\text{Na,K})(\text{Si}_3\text{Al})\text{O}_8$.

5. Conclusions

The porosity of samples increases with increased sodium carbonate content, reaching extremely low values at high percentages (10%) due to the formation of sodium oxide, which fills pores and interstitial gaps. The addition of Na_2CO_3 increased the hardness of the ceramic body due to a reduction in apparent porosity, significantly affecting its resistance to penetration. The increase in compressive resistance represents an improvement in the ability of this porcelain material to withstand the compressive stresses that the tooth is subjected to during application. Despite the relatively low

diametrical strength values due to the low force used to form the samples, which, if increased, could positively lead to an increase in fracture toughness. The change in the thermal expansion coefficient with the added percentage of Na_2CO_3 . The figure indicates that the thermal expansion coefficient increases with the increase in the rate of Na_2CO_3 . From x-ray diffraction, there was a decrease in the mullite phase, where it combines with sodium to form new oxide compounds of sodium, aluminum, and silicon, with the appearance of the boron silicate phase and the albite phase.

Conflict of interest

The authors declare no conflict of interest.

Acknowledgments

The authors would like to thank the University of Technology staff for providing help, advice and support.

References

- [1] Christidis, G. E. (Ed.). (2011). Advances in the characterization of industrial minerals. European Mineralogical Union.
- [2] HEIMANN, R. B., & MAGGETTI, M. (2019). The struggle between thermodynamics and kinetics: Phase evolution of ancient and historical ceramics.
- [3] Ekanema, I. I., & Ikpe, A. E. A systematic review of the trends in ceramic materials and its viability in industrial applications. *J. Mater. Charact. Appl*, 2(2), 63-78.
- [4] Enderle, J., & Bronzino, J. (Eds.). (2012). Introduction to biomedical engineering. Academic press.
- [5] Pollington, S., & van Noort, R. (2009). An update of ceramics in dentistry. *Int J Clin Dent*, 2(4), 283-307.
- [6] Zinovia Surlari, Elena Luca, Dana-Gabriela Budală, Oana Doloca, Țănculescu, Cristina Iordache, Dragoș Ioan Virvescu. (2020). Dental Ceramic -A Literature Review. *Romanian Journal of Medical and Dental Education*, 9(6), pp. 47- 52.
- [7] Okoubulu, A. B., Mgbemere, H. E., Obidiegwu, E. O., & Nwaeju, C. C. (2023). Effect of feldspar and silica variation on the properties of dental porcelain. *Nigerian Journal of Technology*, 42(1), 107-113.
- [8] Kamara, S. (2025). Utilization and Environmental Concerns of $\text{Al}_2\text{Si}_2\text{O}_5(\text{OH})_4$ and its Equilibrium Models in the Adsorption of Toxic Materials: A Review. *J. Mater. Environ. Sci.*, 16 (6), 1138, 1163.
- [9] Abdulmahdi, B. H., & Abdulhussein, F. M. (2025). Geochemistry of the kaolinite-rich claystone in

- Western Iraq. Iraqi Journal of Science, 66(6), 2370-2381.
- [10] Kenneth J. Annsavice "Phillips, science of dental materials" 10th edition W.B. Saunders company. Philadelphia, Pennsylvania, U.S.A. 1996.
- [11] Odewole, P. O., Kashim, I. B., & Akinbogun, T. L. (2022). Investigation into the viability of the properties of porous glass-ceramics produced from granite dust and maize cob for use in thermal insulation of external walls of residential buildings. *Journal of Mechanical Engineering and Sciences*, 16(2), 8943.
- [13] Raut, A. N., & Gomez, C. P. (2016). Thermal and mechanical performance of oil palm fiber reinforced mortar utilizing palm oil fly ash as a complementary binder. *Construction and Building Materials*, 126, 476-483.
- [14] Ali, A., Gaur, A., Pandey, K. K., Tyagi, S., Tarannum, F., Azeem, M., ... & Azeem Sr, M. (2023). Comparative evaluation of compressive and diametral tensile strength in die stone reinforced with different types of nanoparticles: an in vitro study. *Cureus*, 15(6).
- [15] Saleem, S. S., Sabir, S. M., Abdulla, K. A., & Saleem Jr, S. S. (2024). Experimental and finite element analysis of compressive strength and diametral tensile strength of luting cement: An in vitro study. *Cureus*, 16(7).
- [16] Blake, A. (Ed.). (1991). *Handbook of mechanics, materials, and structures*. John Wiley & Sons.
- [17] Sarah M. Alnafaiy, Nawaf Labban, Ahmed Maawadh, Huda A. Alshehri, Abdullah S. Aljamhan, Wejdan Alghamd. (2021). Biaxial Flexural Strength and Hardness of Resin-Matrix Ceramic CAD/CAM Materials, *Ceramics-Silikáty*, 65(3), 285-294.